

Note on spectral form factors in CFTs

Ruihua Fan¹

¹*Department of Physics, Harvard University, Cambridge MA 02138, USA*

July 31, 2020

Abstract

In this note, we study the behavior of spectral form factors in $c = 1$ compact boson CFTs. We focus on its behavior at rational and irrational radius square. We also look at the effect of averaging over moduli space.

Contents

1 Definitions	1
2 Benchmark: GUE random matrix	2
3 Compact boson CFTs	3
3.1 Conventions	3
3.2 Rational v.s irrational	4
3.3 Average over moduli space	5

1 Definitions

Let us define the partition function as

$$Z(\beta + it) = \sum_n e^{-(\beta+it)E_n} \tag{1}$$

where $\beta > 0$ is the inverse temperature regulating the summation. Accordingly, the spectral form factor is defined as

$$g(\beta, t) = |Z(\beta + it)|^2 = \sum_{n,m} e^{-\beta(E_n+E_m)-it(E_n-E_m)} \tag{2}$$

It has the following behaviors in different time regimes:

1. The initial time $t = 0$, $g(\beta, t) = Z(\beta)^2$ counts the number of states (weighted by the Boltzmann factor).

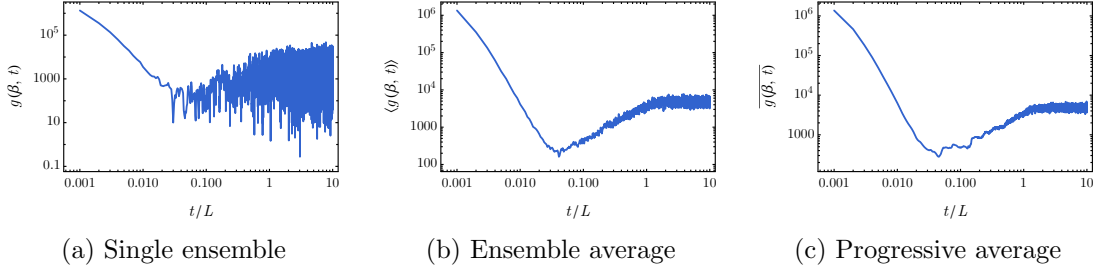


Figure 1: Spectral form factor of GUE random matrix. For all the plots, we choose $\beta = 1, L = 1000$. (a) Single realization of H drawn from the ensemble; (b) Ensemble average over 60 different realizations; (c) Progressive average with $\alpha = 0.9$.

2. The short time regime, $g(\beta, t)$ keeps decaying which is due to the dephasing between different energies.
3. The late time when t is even larger than the smallest energy spacing, only $E_n = E_m$ will make dominant contribution (on an average sense) and $g(\beta, t) \rightarrow Z(2\beta)$, which is much smaller than the initial value.
4. The behavior in the intermediate time regime relies on the detail of the system.

2 Benchmark: GUE random matrix

The GUE random matrix provides one the most canonical demonstration, which we reproduce here. For an ensemble of $L \times L$ Hermitian matrices H , we define the probability distribution as

$$P(H) \propto e^{-\frac{L}{2} \text{Tr } H^2}. \quad (3)$$

The eigenvalues are distributed in the interval $[-2, 2]$ in the large L limit. A typical behavior of $g(\beta, t)$ is shown in Fig. 1. We can see that

- For a fixed realization of H , $g(\beta, t)$ shows rapid oscillation at late time.
- After ensemble average, $g(\beta, t)$ shows the dip-ramp-plateau behavior. The plateau time is around $t \sim L$, which is of the same order of the inverse level spacing and is consistent with our picture above.
- Same behavior is also observed if one performs a time average. Here, we choose the so-called progressive average

$$\overline{g(\beta, t)} = \frac{1}{100} \sum_{k=-50}^{50} g\left(\beta, t + \frac{k}{100}\alpha t\right). \quad (4)$$

The average scheme does not matter.

In the context of GUE, both ensemble average and time average are meaningful. In a generic clean system, it is more natural to consider the time average. For compact boson CFTs, the moduli space provides another average scheme, which can be regarded as an analog with the ensemble average.

3 Compact boson CFTs

In this section, we numerically compute the spectral form factor $g(\beta, t)$ for $c = 1$ compact boson CFTs and focus on two questions:

1. The difference between R^2 being rational and irrational and how the difference emerges as R^2 gradually approaches the irrational limit. [1]
2. The behavior of $g(\beta, t)$ under average over the moduli space. [2]

3.1 Conventions

We follow Polchinski's convention and set $\alpha' = 1$. The action is

$$S = \frac{1}{4\pi} \int d^2\sigma \partial X \bar{\partial} X, \quad X \cong X + 2\pi R \quad (5)$$

States in the Hilbert space corresponds to vertex operators $V_{n,w}$ with conformal weight

$$(h_{n,w}, \tilde{h}_{n,w}) = \frac{1}{4} \left(\left(\frac{n}{R} + wR \right)^2, \left(\frac{n}{R} - wR \right)^2 \right) \quad (6)$$

where n, w characterize the center of mass momentum and winding in space respectively. Here, we focus on the S^1 branch, where n, w are both integers. The torus partition function with modular parameter τ is

$$Z_{S^1}(R, \tau) = \frac{1}{\eta(\tau)\bar{\eta}(\bar{\tau})} \Theta(R, \tau) \quad (7)$$

where $\eta(\tau)$ is the Dedekind eta function coming from the summation over oscillating modes (the quantum part)

$$\eta(\tau) = q^{1/24} \prod_{n=1}^{\infty} (1 - q^n), \quad q = e^{2\pi i \tau}, \quad (8)$$

And $\Theta(R, \tau)$ is the $c = 1$ case of the Riemann-Siegel theta-function coming from the winding along spatial and temporal directions (the classical part)

$$\Theta(R, \tau) = \sum_{n,w} \exp \left[\frac{i\pi\tau}{2} \left(\frac{n}{R} + wR \right)^2 - \frac{i\pi\bar{\tau}}{2} \left(\frac{n}{R} - wR \right)^2 \right] \quad (9)$$

It can also be written in a more compact form

$$\Theta(R, \tau) = \Theta(0|T) = \sum_{n,w \in \mathbb{Z}} \exp \left[i\pi (n-w) T \binom{n}{w} \right], \quad T = \frac{1}{2} \begin{pmatrix} \frac{1}{R^2}(\tau - \bar{\tau}) & (\tau + \bar{\tau}) \\ (\tau + \bar{\tau}) & R^2(\tau - \bar{\tau}) \end{pmatrix}. \quad (10)$$

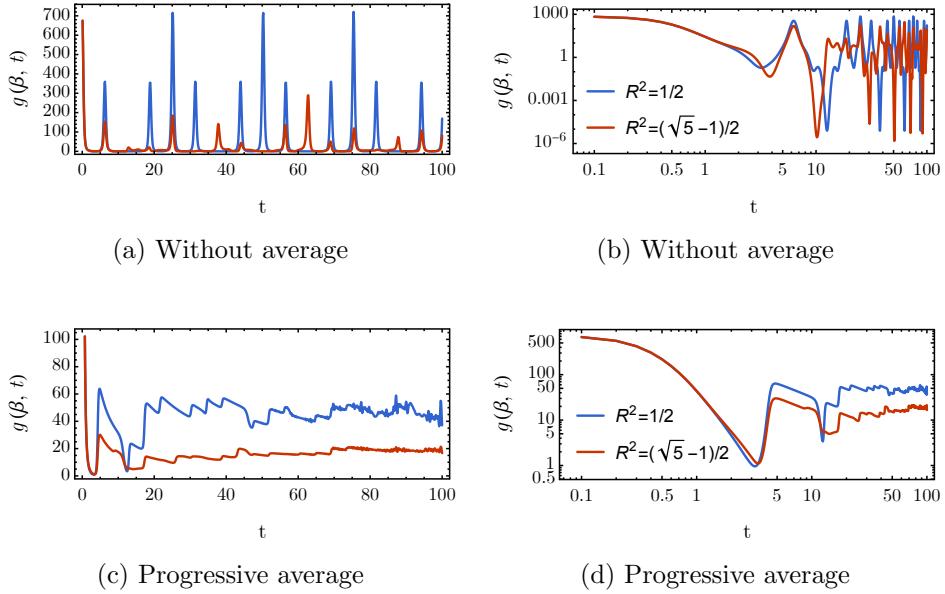


Figure 2: Spectral form factor for $c = 1$ compact boson conformal field theories with radius square being rational v.s. irrational. The red curves corresponds to $R^2 = (\sqrt{5} - 1)/2$, the inverse golden ratio. The blue curves corresponds to $R^2 = 1/2$, the first principal convergent of $(\sqrt{5} - 1)/2$. The progressive average uses $\alpha = 0.9$

Analytically continuing the modular parameters as

$$\tau \rightarrow \frac{i(\beta + it)}{2\pi}, \quad \bar{\tau} \rightarrow -\frac{i(\beta + it)}{2\pi} \quad (11)$$

yields $Z(\beta + it)$ and the spectral form factor accordingly.

3.2 Rational v.s irrational

Now, we look at the difference between rational and irrational R^2 (notice that it is R^2 that enters the spectrum). For a rational R^2 , the spectrum has gap. For an irrational R^2 , the spectrum is expected to be much more dense, and we expect an irregular behavior for $g(\beta, t)$.

The results are shown in Fig. 2. We can see that

1. Without averaging, the spectral form factor is periodic in time with several sharp peaks for rational R^2 and does not show clear recurrence for irrational R^2 .
2. After performing the progressive average, there is not qualitative difference between rational and irrational R^2 . One can also do the time average with a fixed time window, the result is qualitatively the same.

These are consistent with the observation in Ref. [1].

We are also interested in how the behavior of $g(\beta, t)$ changes as R^2 gradually approaches an irrational number. One can simply increase the digits of the rational approximation. A better

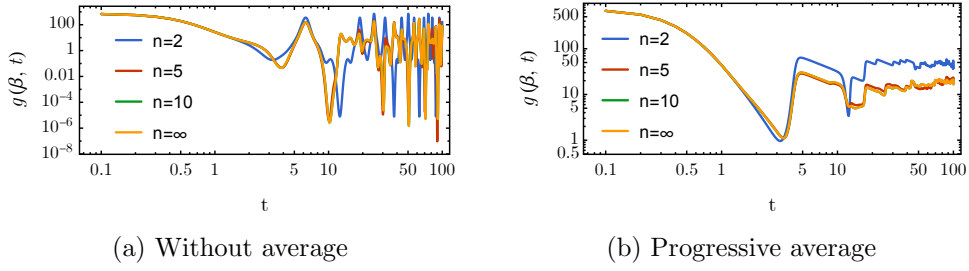


Figure 3: The spectral form factor for $c = 1$ compact boson, as $R^2 = \text{Fib}[n]/\text{Fib}[n + 1]$ approaches the irrational radius square. The progressive average uses $\alpha = 0.9$. The behavior of the curves changes in a continuous fashion with the increase of n .

choice is to use the sequence of the principal convergents generated by the continued fraction representation.¹ Here, we choose the inverse golden ratio $x = \frac{\sqrt{5}-1}{2}$, which has a particularly simple sequence, given by the ratio of two nearby Fibonacci numbers

$$\{x_n = \frac{\text{Fib}[n]}{\text{Fib}[n+1]}\}, \quad \lim_{n \rightarrow \infty} x_n = \frac{\sqrt{5}-1}{2}. \quad (13)$$

The result is shown in Fig. 3. We see that the curve converges to the behavior in the irrational limit without any singularity.

3.3 Average over moduli space

As an analog with the ensemble average for random matrices, we can also average over the moduli space \mathcal{M} of the compact boson, which is parametrized by the radius R . Notice that compact bosons with different R are connected by the exactly marginal perturbation $\delta S = \frac{\delta g}{4\pi} \int d^2\sigma \partial X \bar{\partial} X$, we can use that to define a Zamolodchikov metric for \mathcal{M} as

$$ds^2 = \text{const} \frac{dR^2}{R^2} \propto \delta g^2 \langle \partial X \bar{\partial} X | \partial X \bar{\partial} X \rangle \quad (14)$$

It induces a measure for the moduli space

$$\mu(R) = \text{const} \frac{dR}{R} \quad (15)$$

In our convention, T-duality interchanges R with $1/R$. Therefore, we only have to focus on $R \in (0, 1]$. For the sake of convergence, let us constrain the allowed radius to be $[R_{\min}, 1]$. The normalized measure is

$$\mu(R) = \frac{1}{|\log R_{\min}|} \frac{dR}{R} \quad (16)$$

¹For irrational real number x , we always have an infinite continued fraction representation

$$x = a_0 + \frac{1}{a_1 + \frac{1}{a_2 + \dots}}, \quad a_0 \in \mathbb{Z}, a_j \in \mathbb{Z}^+. \quad (12)$$

The n -th principal convergent is the rational number p_n/q_n obtained by a truncation at a_n

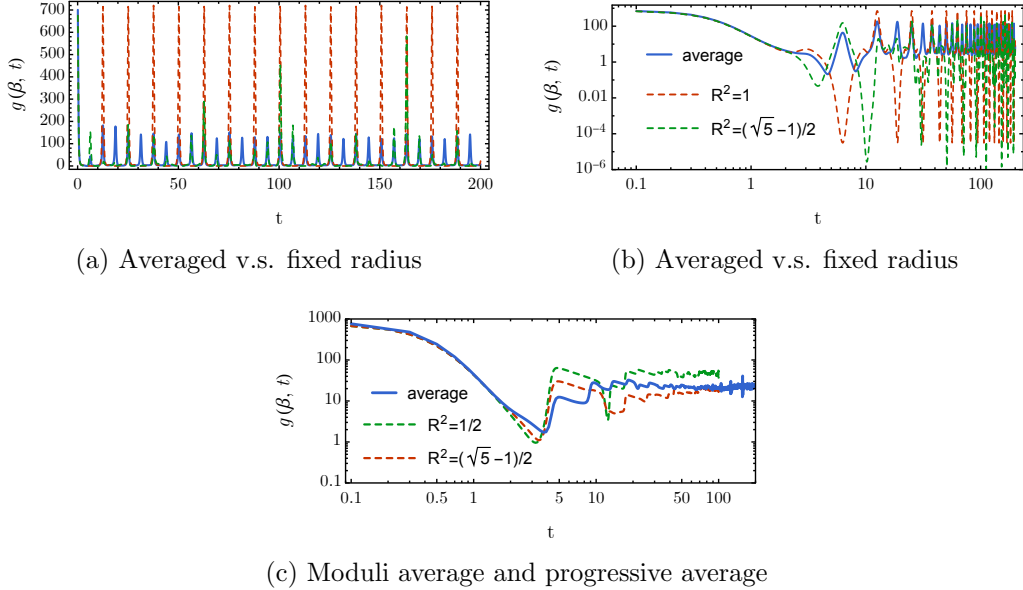


Figure 4: Spectral form factor for $c = 1$ compact boson CFTs averaged over the moduli space $[R_{\min}, 1]$ with $R_{\min}^2 = \frac{\sqrt{5}-1}{2}$. The blue curves are the averaged results and others are for fixed radius plotted for the sake of comparison. When numerically computing the moduli average, we approximate the integral by an summation with $\Delta R^2 = 0.01\sqrt{2}$ for (a) and (b) $\Delta R^2 = 0.05\sqrt{2}$ for (c). In (a) and (b), we compare the moduli average result and $g(\beta, t)$ with $R = R_{\min}$ and $R = 1$. In (c), we compare the moduli average result and ones without doing moduli average (shown in Fig. 2(d)).

We define the averaged spectral form factor as

$$\begin{aligned} \langle g(\beta, t) \rangle &= \int \mu(R) g(\beta, t) = \frac{1}{|\log R_{\min}|} \frac{1}{|\eta(\tau)|^2} \int_{R_{\min}}^1 \frac{d(R^2)}{R^2} |\Theta(R, \tau)|^2 \\ &= \frac{1}{|\log R_{\min}^2|} \frac{1}{|\eta(\tau)|^2} \int_{R_{\min}}^1 \frac{dR}{R} |\Theta(R, \tau)|^2 \end{aligned} \quad (17)$$

As an example, we choose $R_{\min}^2 = \frac{\sqrt{5}-1}{2}$ and numerically compute the average. The choice here is to make connection to the previous discussion. The result is shown in Fig. 4. In (a) and (b), we compare the result for $g(\beta, t)$ after the average over moduli and those with fixed radius square (both rational and irrational). We see that $\langle g(\beta, t) \rangle$ does not become more irregular than $g(\beta, t)$ at irrational radius square. It shows peaks whose magnitudes are close to each other.

Furthermore, we can also perform a progressive time average on top of the moduli average and result is shown in Fig. 4(c). As we can see the peaks disappear and gives way to a plateau at the late time. Comparing to the results shown in Fig. 2(d) (also plotted here together for comparison), the result with both moduli and progressive average becomes smoother as one may expect. Its appearance is closer to the dip-ramp-plateau behavior observed in the GUE case. However, it is hard make a sharp statement.

References

- [1] J. Kudler-Flam, L. Nie and S. Ryu, *Conformal field theory and the web of quantum chaos diagnostics*, *JHEP* **01** (2020) 175 [[1910.14575](#)].
- [2] A. Maloney and E. Witten, *Averaging Over Narain Moduli Space*, [2006.04855](#).